

Can we map the interannual variability of the whole upper Southern Ocean with the current database of hydrographic observations?

Céline Heuzé, Frédéric Vivier, Julien Le Sommer, Jean-Marc Molines, Thierry Penduff

▶ **To cite this version:**

Céline Heuzé, Frédéric Vivier, Julien Le Sommer, Jean-Marc Molines, Thierry Penduff. Can we map the interannual variability of the whole upper Southern Ocean with the current database of hydrographic observations?. Journal of Geophysical Research. Oceans, 2015, 120 (12), pp.7960-7978. 10.1002/2015JC011115 . insu-01351683

HAL Id: insu-01351683

https://insu.hal.science/insu-01351683

Submitted on 4 Aug 2016

HAL is a multi-disciplinary open access archive for the deposit and dissemination of scientific research documents, whether they are published or not. The documents may come from teaching and research institutions in France or abroad, or from public or private research centers.

L'archive ouverte pluridisciplinaire **HAL**, est destinée au dépôt et à la diffusion de documents scientifiques de niveau recherche, publiés ou non, émanant des établissements d'enseignement et de recherche français ou étrangers, des laboratoires publics ou privés.

AGU PUBLICATIONS

JGR

Journal of Geophysical Research: Oceans

RESEARCH ARTICLE

10.1002/2015JC011115

Key Points:
- All methods introduce significant biases when mapping scattered data onto a regular space-time grid
- Small search radii give more accurate values but large radii fill larger parts of the Southern Ocean
- Such mapping methods should not be used to study trends in mixed-layer depth over the last decade

Correspondence to:
C. Heuzé,
celine.heuze@gu.se

Citation:
Heuzé, C., F. Vivier, J. Le Sommer, J.-M. Molines, and T. Penduff (2015), Can we map the interannual variability of the whole upper Southern Ocean with the current database of hydrographic observations?, *J. Geophys. Res. Oceans*, *120*, 7960–7978, doi:10.1002/2015JC011115.

Received 14 JUL 2015
Accepted 12 NOV 2015
Accepted article online 18 NOV 2015
Published online 17 DEC 2015

© 2015. American Geophysical Union. All Rights Reserved.

Can we map the interannual variability of the whole upper Southern Ocean with the current database of hydrographic observations?

C. Heuzé[1,2], F. Vivier[2], J. Le Sommer[3], J.-M. Molines[3], and T. Penduff[3]

[1]Department of Marine Sciences, University of Gothenburg, Gothenburg, Sweden, [2]CNRS, LOCEAN-IPSL, Sorbonne Universités (UPMC Paris 6), Paris, France, [3]CNRS-LGGE, MEOM, Grenoble, France

Abstract With the advent of Argo floats, it now seems feasible to study the interannual variations of upper ocean hydrographic properties of the historically undersampled Southern Ocean. To do so, scattered hydrographic profiles often first need to be mapped. To investigate biases and errors associated both with the limited space-time distribution of the profiles and with the mapping methods, we colocate the mixed-layer depth (MLD) output from a state-of-the-art 1/12° DRAKKAR simulation onto the latitude, longitude, and date of actual in situ profiles from 2005 to 2014. We compare the results obtained after remapping using a nearest neighbor (NN) interpolation and an objective analysis (OA) with different spatiotemporal grid resolutions and decorrelation scales. NN is improved with a coarser resolution. OA performs best with low decorrelation scales, avoiding too strong a smoothing, but returns values over larger areas with large decorrelation scales and low temporal resolution, as more points are available. For all resolutions OA represents better the annual extreme values than NN. Both methods underestimate the seasonal cycle in MLD. MLD biases are lower than 10 m on average but can exceed 250 m locally in winter. We argue that current Argo data should not be mapped to infer decadal trends in MLD, as all methods are unable to reproduce existing trends without creating unrealistic extra ones. We also show that regions of the subtropical Atlantic, Indian, and Pacific Oceans, and the whole ice-covered Southern Ocean, still cannot be mapped even by the best method because of the lack of observational data.

1. Introduction

Despite its prominent role in the climate system, the Southern Ocean has historically been undersampled compared with the rest of the World Ocean, both because of its remoteness and harsh climate. By promoting the deployment at a global scale of automated floats profiling every 10 days, the international Argo program [*Roemmich et al.*, 2009], launched in 2000, has enabled considerable improvement in space-time coverage of the upper 2000 m of the ocean. The improvement is particularly spectacular in the Southern Ocean where the scarce historical database of observations was moreover highly biased toward austral summer [*de Boyer Montégut et al.*, 2004]. The number of floats simultaneously at sea increased regularly since 2000 to reach the initial objective of 3000 units at the end of 2007 [*Roemmich et al.*, 2009].

To date, these observations, jointly with the historical database, have been primarily used to assess the climatological properties and short-term variability of the Southern Ocean, as well as possible long-term trends (refer to Table 1 for a nonexhaustive list of such studies). They have led to tremendous improvement in the climatological description of the mixed-layer depth (MLD) [e.g., *de Boyer Montégut et al.*, 2004; *Dong et al.*, 2008; *Holte and Talley*, 2009; *Schmidtko et al.*, 2013]. Monthly depth estimates were in particular used to investigate the mixed-layer heat budget on different time scales [*Dong et al.*, 2008; *Vivier et al.*, 2010], while other studies have focused on the seasonal salinity budget [*Ren et al.*, 2011]. Hydrographic observations of the Southern Ocean were also used to investigate possible upper ocean heat content and property changes [e.g., *Lyman and Johnson*, 2008; *Gille*, 2008; *Helm et al.*, 2010].

Using the same data set, albeit with a different end date, these authors do not always find consistent results. In fact, analyses based on this data set generally involve mapping scattered observations on a regular geographical grid (see Table 1), and, for subsurface layers, on isobaric or isopycnal levels (e.g., *Schmidtko et al.* [2013] uses isopycnal levels). The error introduced by the limited and nonuniform distribution of Argo

Table 1. Methods Used in the Literature to Map Argo Float Data in the Southern Ocean (Nonexhaustive List)[a]

Reference	Product	Years	Method	Resolution	Decorrelation
Dunn and Ridgway [2002]	Climatology CARS09	Up to 2009	LOESS fitting	0.5° × 0.5°	Bathymetry dependent
Locarnini et al. [2013]	Climatology WOA2013	Up to 2013	OA	1° × 1°	Isotropic, per basin
de Boyer Montégut et al. [2008]	Climatology MLD	1941–2008	kriging	2° × 2°	12°
Dong et al. [2008]	Climatology MLD and S	2000–2008	OA	1° × 1°	5° lon, 2° lat
Schmidtko et al. [2013]	Climatology MLD	Up to 2011	OA improved	0.5° × 0.5°	4° lon, 3° lat, front
Ren et al. [2011]	Seasonal 15 m S	OA	1° × 1°	6° lon, 3° lat	
Boehme et al. [2008]	Monthly T and S	2004–2005	OA improved	0.4° × 0.25°	3° lon, 2° lat, PV
Sallée et al. [2008]	Monthly MLD	Up to 2009	LOESS fitting	0.5° × 0.5°	Not indicated
Sallée et al. [2008]	Weekly SSH	1999–2006	OA	0.3° × 0.3°	2° lon, 1.5° lat
Lyman and Johnson [2008]	OHC trend	1993–2006	OA two scales	1° × 1°	Short scale 1° lon, long 12°
Gille [2008]	T trend	1930–2006	Averaging	N/A	2°
Helm et al. [2010]	T trend	1940–2007	OA	N/A	Not indicated

[a]For consistency, distances (in km) have been converted to degrees longitude (lon) and latitude (lat) at 45°S. See notations for meaning of acronyms.

profiles as well as by the mapping procedure itself (choice of method and resolution of the final product) may seriously impede the analyses.

Fifteen years after the onset of the Argo program, and with a growing number of buoy deployments in the Southern Ocean over recent years, it becomes timely to investigate to what extent interannual variations of the upper ocean properties can be described with the available space-time coverage. Estimating errors induced by the mapping methods, determining the optimum method and space-time resolution, and assessing which (if any) region of the Southern can still not be mapped accurately are the goals of this paper. Following *Juza et al*. [2012], these questions are examined using 10 years worth of output from a 1/12° global simulation, subsampled using the actual positions and dates of available hydrographic profiles. We focus on the MLD field as a case study.

This article is organized as follows. Both hydrographic and model data are presented in section 2 along with the diagnostics that are performed. The mapping methods that we test are described in section 3. Section 4 explains and discusses the results regarding both the interannual variability and decadal trends. Because of the strong seasonal cycle in MLD, we concentrate on the interannual variability of the deep winter MLD and the shallow summer MLD separately. These results are summarized along with limitations and possible solutions in section 5.

2. Data and Diagnostics

2.1. EN4 Hydrographic Profiles

We use the quality checked global Met Office Hadley Centre EN4 data set of ocean temperature and salinity profiles from January 2005 to December 2014 [*Good et al*., 2013]. It contains most hydrographic profiles available to date, including in particular CTD casts, XBT, and profiling floats. Data compiled in EN4 originate from different databases, primarily the World Ocean Database 2009, the Global Temperature and Salinity Profile Program (GTSPP), and the Argo Program (see detailed description by *Good et al*. [2013]). The profiles are grouped in monthly files that also contain quality information. A quality check flag is provided with each profile, with zero indicating a reliable profile. Within each profile, each depth level has its own quality check value indicating a missing value (0), a reliable value (1), or a spurious value (4, for example a spike in the profile). The quality checks are described by *Ingleby and Huddleston* [2007].

This quality control allowed us to remove profiles that are not deemed reliable, i.e., whose overall profile flag is different from zero. Then, we considered only the depth levels whose parameter flag for temperature, salinity, and depth was equal to 1. We kept only the profiles with a maximum depth larger than 500 m. The MLD is usually computed from density profiles, based on a density difference from a shallow reference depth [*de Boyer Montégut et al*., 2004; *Holte and Talley*, 2009]. We therefore removed the levels where temperature or salinity is missing, hence density not available, and did not consider the profiles where the reference, shallowest value is deeper than 15 m. We saved the latitude, longitude, and date of all the remaining profiles (more than 4000 per month).

The EN4 profiles are irregularly distributed through space and time (Figure 1). Most parts of the Southern Ocean never have more than five profiles per month in a 1° grid cell (Figure 1a). The permanently ice-

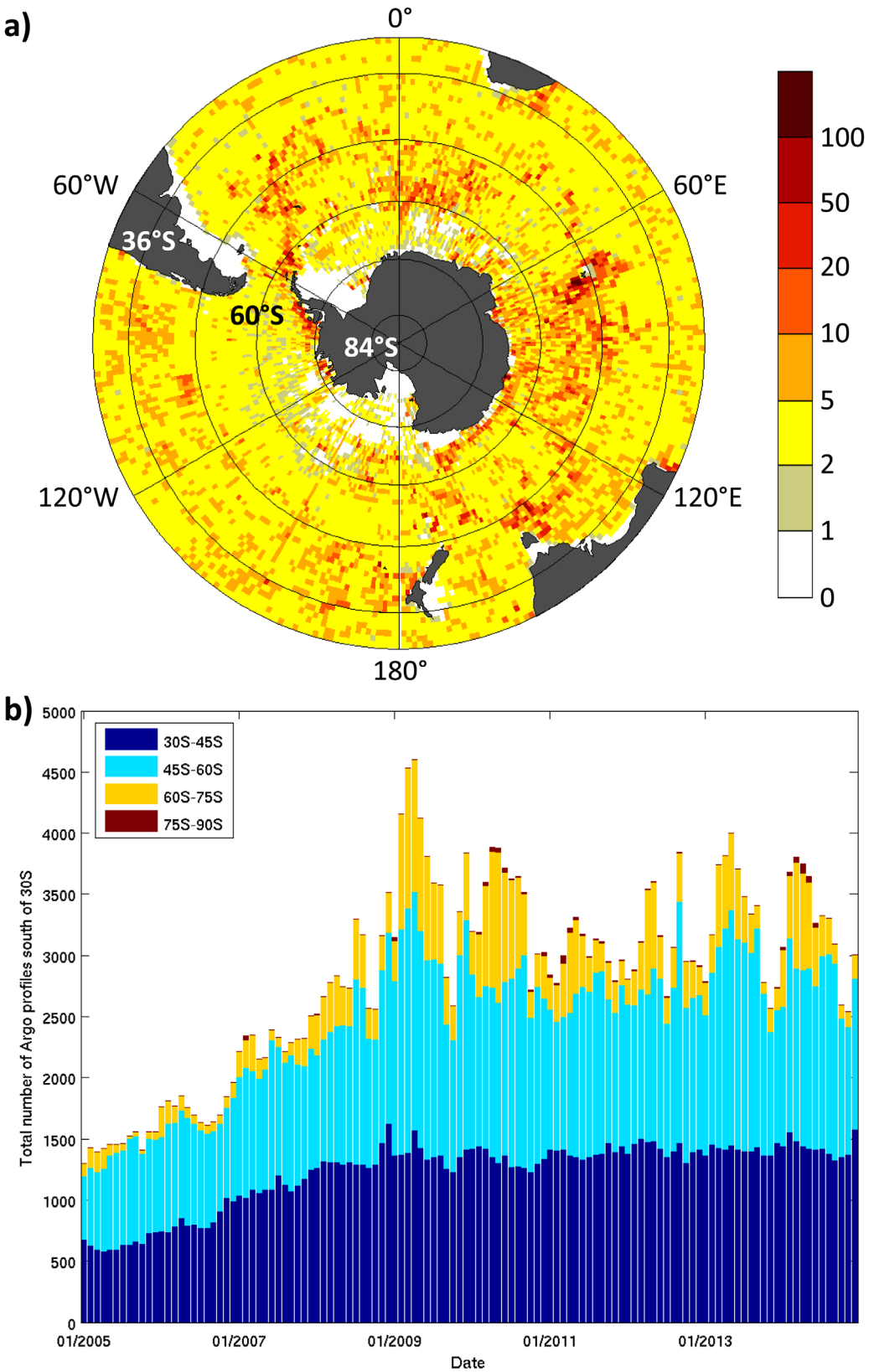


Figure 1. Southern Ocean south of 30°S (a) for each 1° × 1° grid cell, maximum number of EN4 hydrographic profiles containing both temperature and salinity measurements ever reached during a month between January 2005 and December 2014 (logarithmic scale); (b) distribution of these hydrographic profiles per month and latitude band.

covered regions around Antarctica have no profiles. The region between approximately 45°S and 60°S, hereafter referred as "the ACC" for it lies approximately in the Antarctic Circumpolar Current path, is the one with the largest numbers of profiles (Figure 1a). That is confirmed by looking at the distribution of these profiles per latitude band (Figure 1b): north of 60°S is where most profiles lie, although there have been about 1000 profiles between 60°S and 75°S since 2009. Profiles are irregularly distributed with time as well, with a number of available profiles ramping up between 2005 and 2009 with an increased number of Argo float deployment (Figure 1b). Note that there is also suggestion of a seasonal cycle. There are less profiles in winter as ships do not venture in Antarctica and Argo floats cannot deal with the sea ice cover. Can this irregular distribution through both space and time be brought onto a regular grid at regular time steps?

Examination of the actual distribution of hydrographic profiles from EN4 provides some guidance on typical scales to consider for mapping. For each month, after reducing the data set to a 1° grid, we have computed the distance to the nearest nonempty grid cell, both in longitude and latitude. On average through the 10 years 2005–2014, the minimum distance between two profiles of the same month is 3.1° in longitude and 3.5° in latitude, although there are vast areas where this distance is larger (divergence zones) or no data available (typically sea ice). That means that the mapping methods that we use should have a search radius larger than 3°, or they will not always be able to find profiles with which to work, and hence will return no value or relax to a background field depending on the methods. Note that this distance between two simultaneously available profiles has evolved through the last decade from 4.7° in 2005 to 3° in 2009 remaining stable afterward, mirroring the evolution of the number of available hydrographic profiles (Figure 1b).

2.2. DRAKKAR Model

We make use of a 1/12° global ocean/sea-ice simulation performed by the DRAKKAR group and referred to as ORCA12.L46-MJM189. Its very high resolution is particularly adapted to our study as this simulation is eddy-resolving and hence can reproduce the fine-scale, chaotic features of the real ocean. It is based on the Nucleus for European Modeling of the Ocean (NEMO version 3.5) [*Madec*, 2008] model with a 46 level vertical discretization, a partial cell representation of topography, an energy/enstrophy conserving momentum advection scheme [*Penduff et al*., 2007; *Le Sommer et al*., 2009], a total variance diminishing (TVD) tracer advection scheme, an isopycnal Laplacian tracer diffusion operator, a vertical mixing scheme based on the TKE turbulent closure model [*Blanke and Delecluse*, 1993], and a convective adjustment scheme based on enhanced vertical mixing in case of static instability.

The 1958–2012 atmospheric forcing, referred to as the DRAKKAR Forcing Set (DFS5.2) [*Dussin et al*., 2014], is based on ERA-Interim [*Dee et al*., 2011] for the period 1979–2012 (3 hourly 2 m temperatures and humidity, 3 hourly 10 m wind components, daily precipitations and radiative fluxes). In making DFS5.2, ad hoc corrections [*Dussin et al*., 2014] to ERA-Interim were done in order to better fit some observational data set. For the period 1958–1978, ERA-40 [*Uppala et al*., 2005] temperature, humidity, and winds were rescaled according to the 1979–2012 DFS5 forcing set. Precipitation and radiative fluxes are daily climatologies (there is no interannual variability) of the 1979–2012 period. For temperature, humidity, and winds, 3 hourly period was maintained, by interpolating the original ERA-40 6 hourly variables.

We use 10 years of simulation, ranging from 1992 to 2001. Although these years are not the same as the ones for the EN4 data (2005–2014), it does not matter; we do not aim at seeing whether the simulation accurately represents the real ocean, only whether re-mapped data have the same variability as the original field. As a consequence, we make 1 January 1992 in the model correspond to 1 January 2005 in the observations. Having accounted for this 13 year shift, we then colocate the data: for each latitude, longitude, and date for the EN4 profiles, we find the closest latitude-longitude grid cell and day of year in the model. We allocate the MLD value from the model to the matching latitude, longitude, and date of the EN4 profile.

2.3. Resolutions and Tests

The objective is to reconstruct the original MLD field from the model from the subsampled colocated MLD data set. In particular we want to assess:

1. Which method is most appropriate to map scattered hydrographic measurements in the Southern Ocean (Figure 1).
2. Which resolution is optimum for such a mapping.

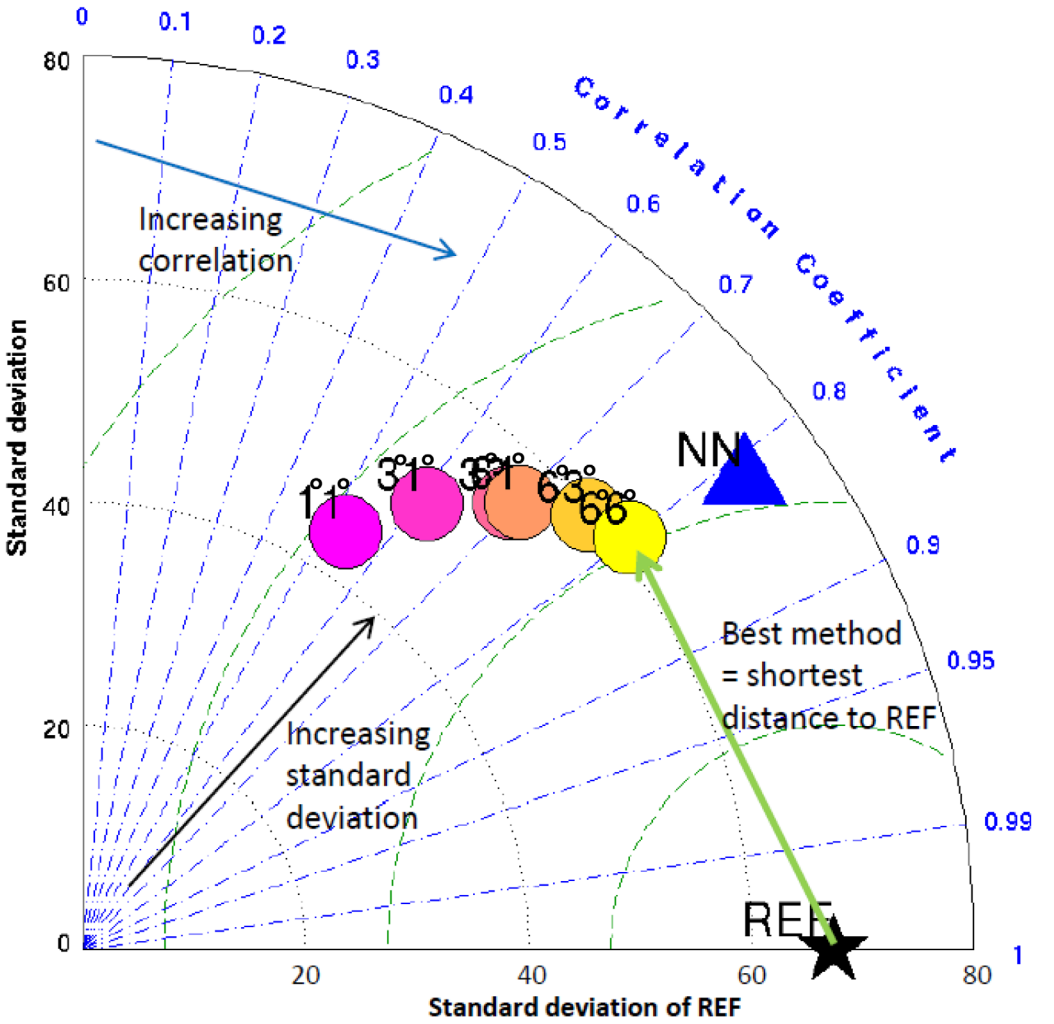


Figure 2. Simplified explanation of a Taylor diagram: the reference REF (in this study, the original model field) is on the *x* axis, and the best method is the one whose point is closest to REF. That depends mostly on its standard deviation (black labels and circles) and its correlation coefficient with REF (blue labels and lines). Numbers next to the colored circles indicate the decorrelation radii of each Objective Analysis (OA) method (e.g., 6°3° for 6° in longitude and 3° in latitude).

To do so, we test three spatial latitude-longitude resolutions (0.5°, 1°, and 2° in both latitude and longitude) and three temporal resolutions (15, 30, and 60 days), which combine in nine spatiotemporal resolutions. For each mapping method (see below), the MLD field is reconstructed at the nine spatiotemporal resolution and compared to the original field from the model. For consistency, model outputs are first degraded from the original 1/12°–5 days resolution to each of the target resolution by taking the median value of the original time steps and latitude-longitude cells included in the new, lower resolution.

Regarding the metrics, we use Taylor diagrams [*Taylor*, 2001] to assess the similarities between the re-mapped fields and the original model output (referred to as "REF" in the figures). The aim is to find the optimum method that has the highest temporal correlation with the original model, the smallest RMS difference with the model, and the closest standard deviation to that of the reference [*Taylor*, 2001] (Figure 2). Taylor diagrams will be shown for the domain average of these quantities. To then distinguish the temporal and spatial performances of the methods, we consider two other diagnostics. For each time step, we calculate the area-weighted mean error between the re-mapped field and the model, that is (method-model)/model. It indicates to what extent the method underestimates or overestimates the MLD in a way that is not biased by the seasonal cycle in MLD. Then for each grid cell, we compute the percentage of time steps where the method cannot return a value or returns a value whose error is larger than 25% (we discuss other values of errors as well). That shows whether there are areas where the methods are unable to correctly

remap the MLD. In particular, we are interested in the areas of Figure 1 where there is hardly any measurement (subtropical Pacific Ocean and Indian Ocean for example).

The first focus is to assess our ability to map the interannual variability. To do so, we examine how well we can reconstruct the interannual variability of the year-round MLD (hence including all the MLD data). As the year-round MLD has a strong seasonal cycle (up to several hundred meters), we also study the interannual variability of the annual extremes: the winter MLD (defined as the time step containing 1 September) and summer MLD (defined as the time step containing 1 March). The second focus is on the methods' ability to reconstruct possible regional trends present in the 10 year data set. These are determined using a least squares fitting method through (1) the annual mean MLD and (2) summer MLD as defined above. The choice of these time series is further detailed in section 4. Following for example *Lyman and Johnson* [2008], we consider only the trends within 95% confidence intervals of the slopes of the linear fits. Following for example *Santer et al.* [2000], the trends in the methods are not significantly different from that of the model REF if there is an overlap in their 95% confidence intervals. This analysis will also highlight spurious trends in the re-mapped data that have been created by the mapping process.

3. Mapping Methods

3.1. Nearest Neighbor (NN)

The first method that we use is a basic nearest-neighbor (NN) interpolation. For each latitude-longitude target grid point and each target date, we consider profiles located in the area defined by the grid cell and its immediate neighbors. If there is no profile the MLD is set to NaN. Otherwise it is set to the median MLD value of available profiles. If, however, a subset of profiles has the same date, only the one closest to the target latitude-longitude is retained prior to computing the median. Note that because the search region is limited to immediate neighbors, the actual coverage of the maps thus obtained is relatively low (see section 4).

In this application, no attempt was made to estimate uncertainty attached to the remapped field, since we know its original value. This would however be recommended when working with the actual EN4 profiles rather than model output.

3.2. Objective Analysis (OA)

The second method that we study, widely used by authors working with Argo data (Table 1), is the objective analysis (OA), introduced in oceanography by *Bretherton et al.* [1976]. This method assumes a known functional form for the covariance of the field to be mapped, and further assumes that the measurement error and the signal are not correlated. Here measurement error is assumed to be a white noise while the correlation function $C(\Delta lon, \Delta lat)$ of the signal is taken as Gaussian, depending on space only to avoid unnecessarily heavy computing:

$$C(\Delta lon, \Delta lat) = \exp\left[-\left(\frac{\Delta lon}{R_{lon}}\right)^2 - \left(\frac{\Delta lat}{R_{lat}}\right)^2\right]. \quad (1)$$

Δlon and Δlat are the distances to the target point in longitude and latitude, respectively, and R_{lon} and R_{lat} are the decorrelation radii in longitude and latitude, respectively. The time dimension is taken into account in a preliminary data reduction step where we retain in each target grid cell the median MLD of all available profiles during the corresponding time step. As part of this preliminary step we also temporarily remove the climatological seasonal cycle of the MLD (directly estimated from the model), since OA is designed to map anomalies [*Bretherton et al.*, 1976]. This climatology is subsequently reintroduced before any analysis is performed. OA returns the best least squares linear estimator of the MLD at each grid cell of the domain together with a formal estimate of the associated error variance. All nonempty grid cells enter the calculation but in practice profiles located further than two decorrelation radii from the target grid cell have virtually no impact on the solution. These are therefore ignored to reduce computing time, i.e., we limit the search radius to two decorrelation radii.

We test three values for each decorrelation radius (1.5°, 3°, and 6°), based on the range of values used in the literature (Table 1), and consistent with the 3° interprofile average distance we have estimated. For consistency with the literature, and bearing in mind the predominantly zonal nature of Southern Ocean fields, we

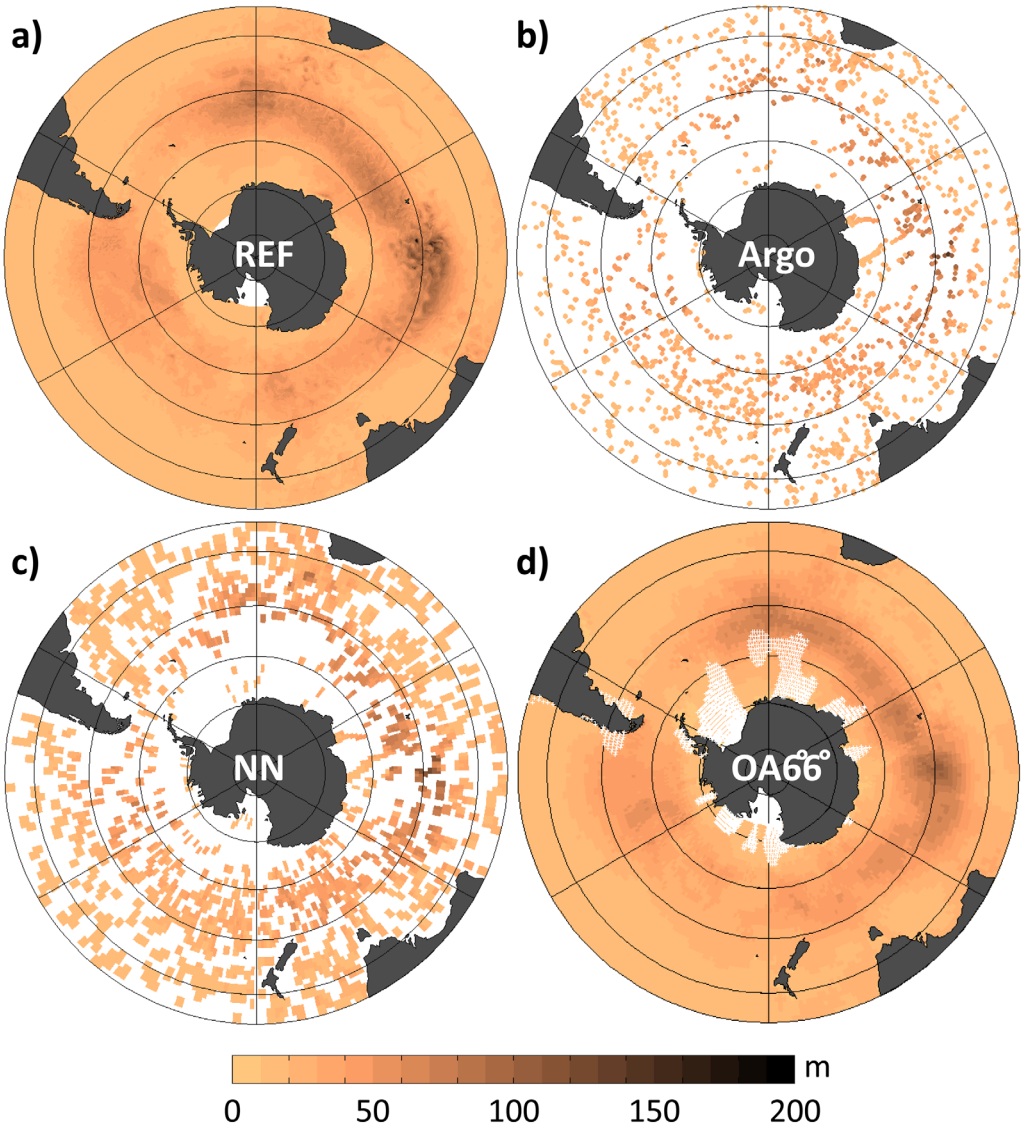


Figure 3. January 2014, Southern Ocean south of 30°S, target resolution of 30 days and 1° horizontally, (a) model MLD (REF); (b) model MLD at the location of EN4 observations; (c) MLD remapped using the nearest neighbor (NN) method; (d) MLD remapped using an objective analysis (OA) with both latitude and longitude decorrelation radii equal to 6°. White stappling in Figure 3d indicates where the OA formal error is larger than 80%, i.e., points discarded from our analysis.

consider only the cases where the longitude radius is larger or equal to that in latitude. For each of the nine spatiotemporal target resolutions, we compare the six combinations of radii and assess which one is most appropriate to that resolution. Hereafter, we refer to the cases as "OA[rounded decorrelation radius in longitude]° [rounded decorrelation radius in latitude]°." For example, OA6°1° corresponds to a radius of 6° in longitude and 1.5° in latitude.

We discard (set to NaN) points where the formal error returned by OA is larger than 80% of the signal variance. We recommend a similar practice when working with the actual EN4 hydrographic data and their associated errors.

The different methods are illustrated in Figure 3, shown for the example of January 2014 and the resolution 30d, 1°. Starting from the model output (Figure 3a), we extract the location of the Argo floats for these 30 days and attribute to them the corresponding model MLD value (Figure 3b). We then remap the data, using NN (Figure 3c) or OA (Figure 3d, example with both radii equal to 6°, white stappling indicates a formal error larger than 80%).

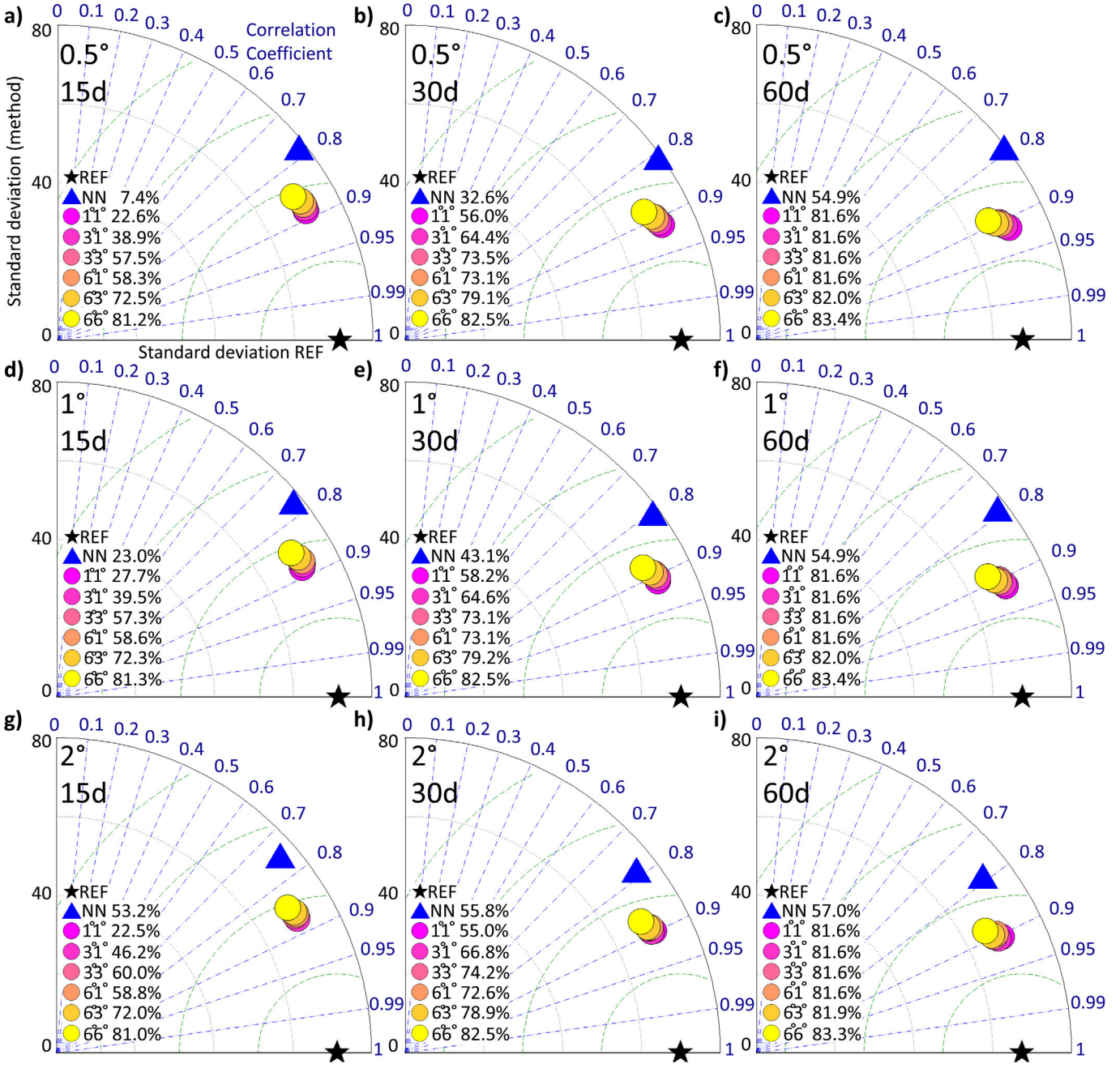


Figure 4. Taylor diagrams in the Southern Ocean south of 30°S, for all the resolutions, when considering the MLD of all the months between January 2005 and December 2014. In the legends, numbers next to the colored circles indicate the decorrelation radii of each OA (e.g., 6°3° for 6° in longitude and 3° in latitude), and percentages indicate the fraction of the Southern Ocean area for which each method returns values.

4. Results

4.1. Interannual Variability

4.1.1. Overall Performance of the Mapping Methods

We assess the performances of the seven re-mapping methods (OA with six combinations of decorrelation radii and NN) for nine spatiotemporal resolutions using Taylor diagrams. These provide the distance to the reference field REF, considering only the grid cells with a non-NaN value (i.e., for OA, grid points with a formal error lower than 80%). Hence, along with Taylor diagrams we also study the actual coverage or filling rate of the mapping method, expressed as a fraction of the Southern Ocean's area. We examine the reconstruction of the year-round, winter, and summer MLD.

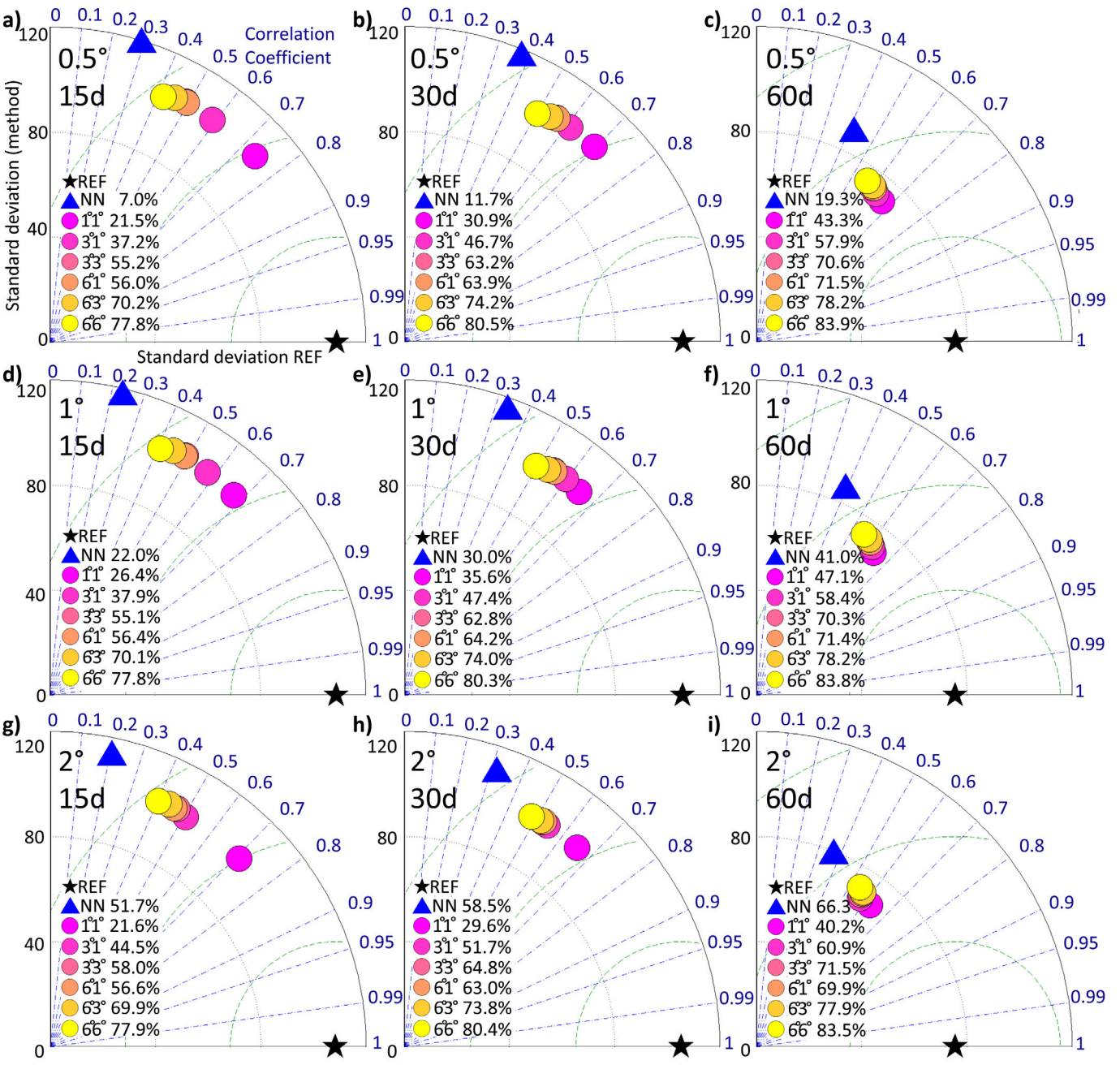


Figure 5. Same as Figure 4 except for the winter MLD.

4.1.1.1. Year-Round MLD

When considering all the months (Figure 4), the best method, that is the one whose point is closest to REF, is always OA1°1°, although all OAs are relatively close to each other. That is because they all simulate similar seasonal cycles, hence have similar correlations with REF (shown in blue, the angle from the vertical axis). For all OAs, their standard deviation (given by their distance to the center) is near-equal to that of REF (*x* axis), also because of similar seasonal cycles. All OAs perform best with a resolution of 60 days (Figure 4, right column): the lower the temporal resolution, the more points OA has to compute its field, hence the more accurate it is likely to be. The resolution also controls the fraction of the Southern Ocean where values are returned by the methods. For all methods, this fraction increases as the temporal resolution (and spatial resolution to a lesser extent) decreases. For all resolutions, larger decorrelation radii correspond to a higher

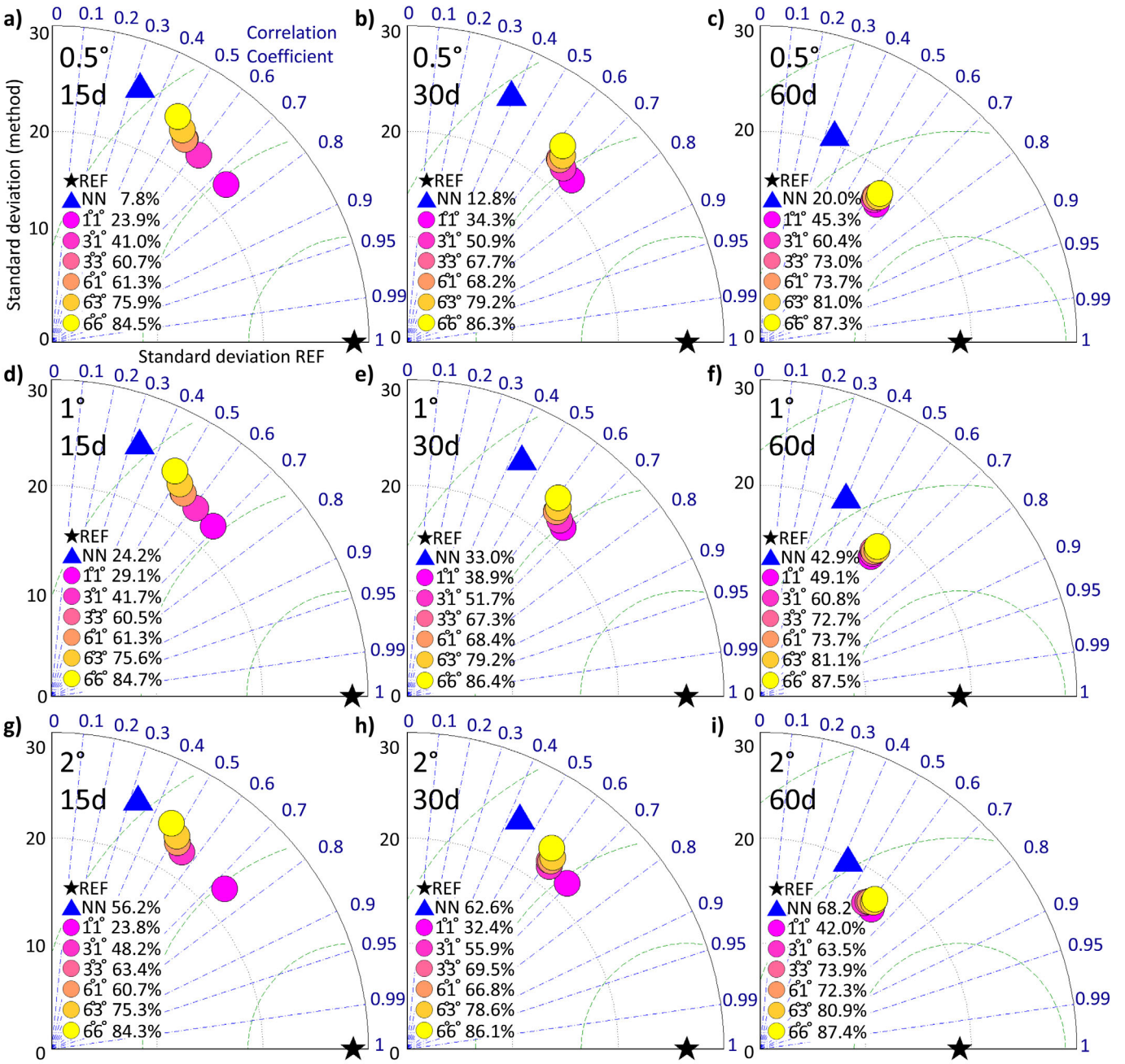


Figure 6. Same as Figure 4 except for the summer MLD.

filling rate as was expected from the larger search radii. For example, OA6°6° always returns values for more than 81% of the Southern Ocean (Figure 4, yellow dots). At low temporal resolutions (60d), all OAs fill more than 81% of the map, regardless of the decorrelation radius. A temporal resolution of 60 days returns relatively accurate values and a high filling rate for all OAs.

4.1.1.2. Winter and Summer MLD

As the high correlations of the year-round MLD (Figure 4) are attributable for a large part to the strong seasonal cycle in MLD, we now study the interannual variability of winter only (Figure 5) and summer only (Figure 6). Considering only the interannual variability of one season (i.e., winter or summer) we find again that OA is more accurate than NN and that OA1°1° performs best (Figures 5 and 6). Performances are overall degraded compared with the mapping of the year-round MLD owing to the absence of the dominant

Table 2. Comparison of the Methods NN, OA1°1°, and OA6°6° for All the Resolutions[a]

	0.5°			1°			2°		
Criteria	15d	30d	60d	15d	30d	60d	15d	30d	60d
Mean NN	5.2	2.8	1.5	5.1	2.8	1.4	5.1	2.8	0.9
Mean OA1°1°	5.2	4.3	4.0	5.1	4.2	4.0	5.2	4.3	4.0
Mean OA6°6°	5.5	4.4	4.1	5.3	4.3	4.0	5.1	4.2	3.9
Median NN	9.3	7.1	7.5	9.8	8.9	7.9	10.3	9.9	7.7
Median OA1°1°	6.0	6.1	6.2	5.6	5.5	5.6	6.5	6.5	6.2
Median OA6°6°	8.8	8.6	8.3	8.6	8.3	8.2	8.4	8.6	8.2
Max NN	30.2	24.3	17.9	29.2	23.4	17.8	27.6	21.2	18.0
Max OA1°1°	21.6	20.7	20.7	20.5	20.0	20.0	21.5	21.5	21.5
Max OA6°6°	27.3	27.3	27.3	26.9	26.9	26.9	26.1	26.1	26.1
Min NN	−28.9	−27.9	−23.5	−27.8	−28.2	−25.3	−28.0	−27.7	−27.4
Min OA1°1°	−14.1	−15.5	−15.6	−12.5	−14.2	−14.8	−15.5	−15.5	−16.1
Min OA6°6°	−21.2	−21.2	−21.2	−21.6	−21.6	−21.6	−22.5	−22.5	−22.5

[a]Mean, median, maximum (max) and minimum (min) between 2005 and 2014 of the area-weighted mean error (in %), defined as the difference (method-model) divided by the value of the model at each grid cell.

seasonal cycle. In winter, the standard deviation of the methods and REF are larger than that of the year-round MLD (maximum of 120 m in winter, Figure 5, compared to 80 m year-round, Figure 4), as we consider only the deep winter MLD. For the methods and REF alike, the standard deviation in winter is strongly reduced with a temporal resolution of 60 days (minimum of 60 m for OA1°1°, right column of Figure 5). The standard deviation of the summer MLD in contrast is smaller than that of the year-round MLD (maximum of 30 m for REF, Figure 6) as we consider only the shallow summer values. For all methods and REF, the standard deviation decreases with the temporal resolution (minimum of 15 m for 60 days and OA1°1°, right column of Figure 6) whereas the spatial resolution had no significant effect. For both seasons, all OAs improve both in accuracy and coverage as the temporal resolution decreases (Figures 5 and 6) and that more data are available at each time step. Likewise, for all spatial resolutions, the differences in performance between the methods decrease (their points are closer on the figures) with the temporal resolution. In fact, solutions for large decorrelation radii are less influenced by the occasional extreme values that might be picked up

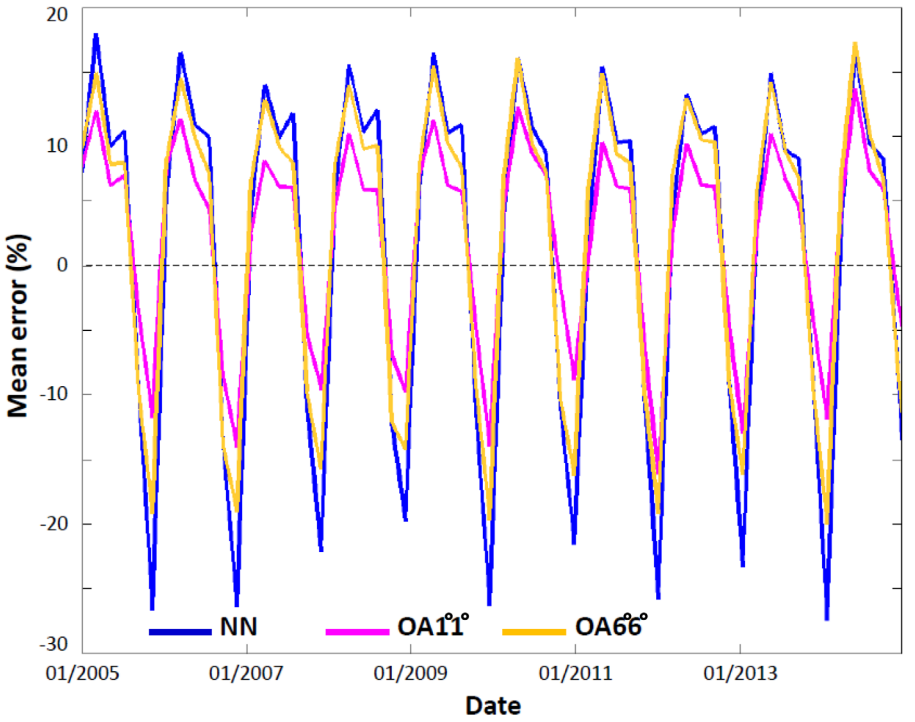


Figure 7. Resolution 60 days and 2° horizontally, time series of the area-weighted mean error (method-model)/model over the Southern Ocean south of 30°S for the method NN (blue), OA1°1° (magenta, both decorrelation radii equal to 1.5°) and OA6°6° (orange, both equal to 6°).

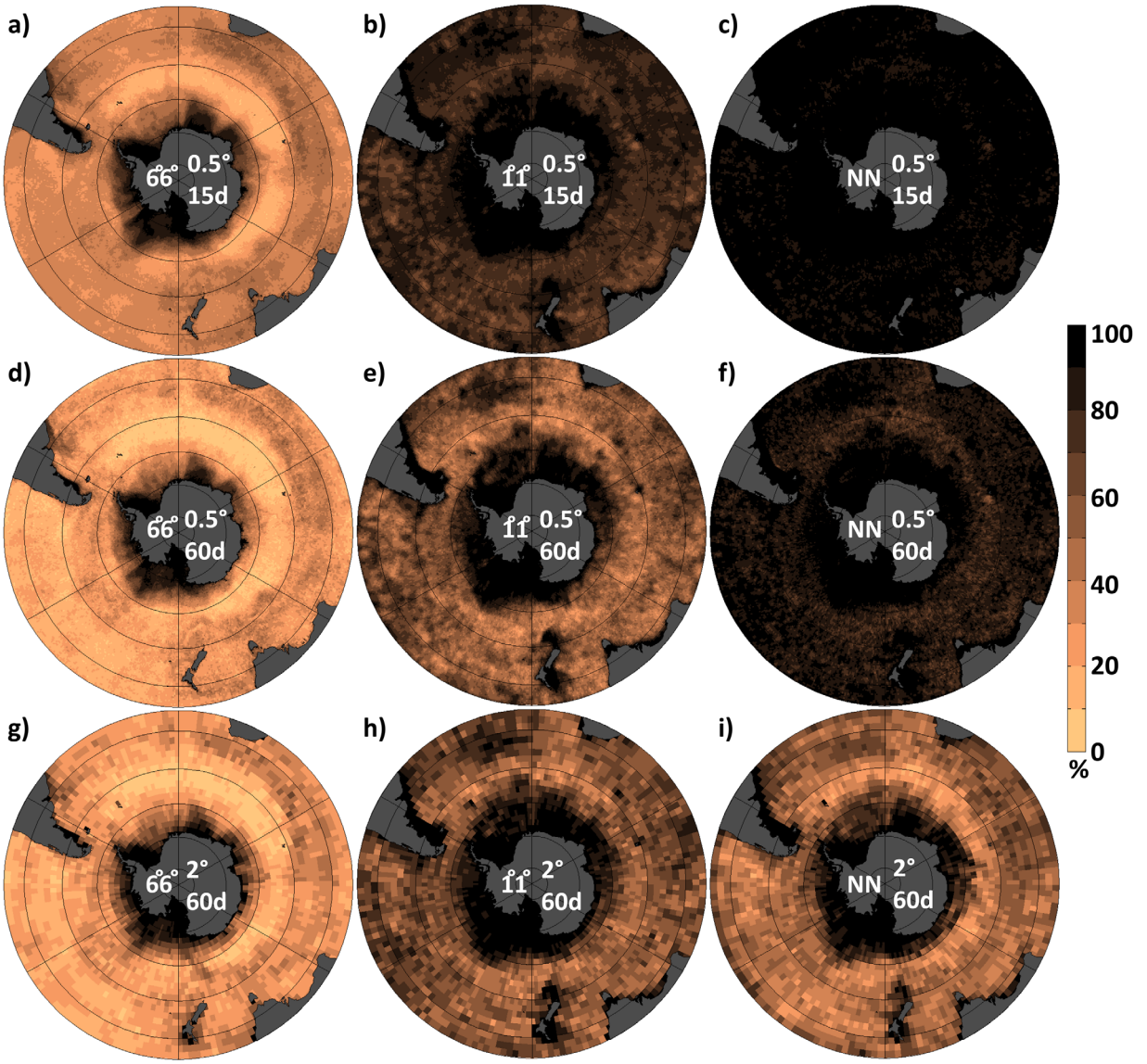


Figure 8. Southern Ocean south of 30°S, for the methods OA6°6° (left, both decorrelation radii equal to 6°), OA1°1° (center, both equal to 1.5°), and NN (right), for each grid cell, percentage of time steps with an error larger than 25% or no value, for two spatial (0.5 and 2°) and temporal (15 and 60 days) resolutions.

with their extended search radius, as these are likely to be attenuated by the availability of additional data thanks to the longer time periods. Similarly, NN becomes less inaccurate as the spatial resolution decreases and hence each grid cell is more likely to have (good) data. Again, OA6°6° with a temporal resolution of 60 days is the method that returns values for most of the Southern Ocean (filling rates on right column in Figures 5 and 6), and the spatial resolution has little impact on the result. For OA, it is the search area controlled by the decorrelation radii that matters (consistent with our remark in section 2) as well as the number of points available at each time step, whereas NN needs a coarser grid to find points to work with. With a spatial resolution of 2°, NN has a higher filling rate than OA1°1° and OA3°1° (bottom row of Figures 5 and 6) but is less accurate.

4.1.2. Temporal and Spatial Structure of the Error

Until the end of this section on the interannual variability, only OA1°1° (most accurate of the OAs), OA6°6° (highest filling rate) and NN are used. To evaluate the performances of these three methods for mapping the year-round MLD through the 10 year period 2005–2014, we compute the area-weighted mean errors of each time step for all the resolutions. Note that the error at each grid point is expressed in % and defined as (method-model)/model. We compare the mean, median, maximum, and minimum of these errors through

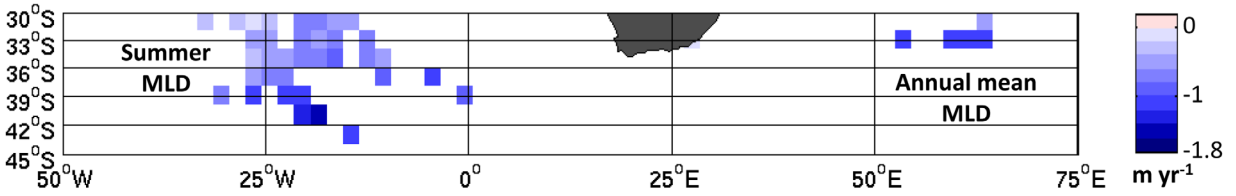


Figure 9. Significant trends in the model used in this paper: in the Atlantic Ocean for the summer MLD, and in the Indian Ocean for the annual mean MLD, both shown on the same figure.

time (Table 2). The mean (median) relative bias is consistently slightly positive ranging from 1 to 6% (6–9%) depending on the mapping methods and resolutions: on average, the MLD is slightly deeper after remapping than in the model. For all three methods, the mean and median errors decrease along with the temporal resolution (first six rows of Table 2). This further confirms our previous results on the importance of the number of points available for all methods. The impact of the spatial resolution is less consistent: for NN, the maximum error tends to decrease along with the spatial resolution (as expected from our previous results), but the minimum error (i.e., largest underestimation) becomes worse as the spatial resolution decreases. The spatial resolution has little impact on the OAs. Finally, none of the methods performs obviously better than the others: NN has the smallest mean and minimum errors, OA1°1° the smallest median and maximum. Similarly, no resolution outperforms the others. Based on the previous results from Figures 4–6, a resolution of 2° and 60 days is used for the three methods now.

So far, we have found that no method performs better than the others on all aspects and that the choice of the method depends on whether accuracy or large map coverage is to be privileged. These results were found when studying both the whole time series (Figure 4) or the annual extremes (Figures 5 and 6). We now study the impact of the choice of method on the seasonal cycle (Figure 7). We find the same results as previously: there are less differences between the methods in summer (positive peaks in Figure 7) than in winter (negative peaks in Figure 7). All three methods have a similar seasonal cycle, underestimating the MLD in winter (negative error ranging from −10 to −25%) and overestimating it in summer (positive error ranging from 10 to 18%, Figure 7). That is, deep winter MLDs are not deep enough, and shallow summer MLDs are not shallow enough. All methods appear to be smoothing the original data set too much, leading to an underestimated seasonal cycle. This explains why considering the whole time series returned better values than the annual extremes: the error oscillates around zero throughout the year. Despite the increase in coverage between 2005 and 2009 (Figure 1), the mean error is fairly constant over the 10 years.

We have shown which of the methods is most relevant depending on which use is to be made of the data (and which resolution targeted). One last aspect has to be taken into account though: the spatial coverage of each method, and in particular the regions where they perform best. For three resolutions, for each grid cell, we compute the percentage of time steps where a value is returned by the methods and that the error associated with this value is lower than 25% (Figure 8). Here the results are striking, with OA6°6° returning accurate values nearly half of the time outside of the ice-covered region even at high resolution, and OA1°1° and NN failing to reach a similar level of accuracy even at the lowest resolution. All three methods perform the least well in the areas that have little measurements, mostly the ice-covered region around Antarctica, the Subtropical Front in the Atlantic and Indian Oceans (around 41°S), and the subtropical Pacific

Table 3. Trends and Their 95% Confidence Interval (in m yr^{-1}) in Summer MLD in the Atlantic Ocean[a]

Resolution	REF	OA1°1°	OA3°1°	OA3°3°	OA6°1°	OA6°3°	OA6°6°	NN
0.5° 15d	−1.20 ± 0.69					0.88 ± 0.04		
0.5° 30d	−0.87 ± 0.28							
0.5° 60d	−0.60 ± 0.30		−0.30±0.29*	−0.53±0.49*	−0.37±0.30*	−0.51±0.20*		
1° 15d	−1.34 ± 0.61							
1° 30d	−0.87 ± 0.27							
1° 60d	−0.61 ± 0.31		−0.39±0.09*	−0.58±0.31*		−0.53±0.08*	−0.68±0.06*	
2° 15d	−1.34 ± 0.61							
2° 30d	−0.86 ± 0.21							
2° 60d	−0.60 ± 0.31		−0.25±0.10*	−0.44±0.18*	−0.34±0.04*	−0.44±0.09*	−0.46±0.11*	−0.49±0.36*

[a]Only significant trends are indicated. A star ⋆ indicates that there is a partial overlap between the REF and method's intervals.

Table 4. Common Area Between REF and Each Method (in 10,000 km^2) for the Summer MLD, and Ratio Between the Area With a Trend in REF But Not in the Method, and the Area With a Trend in the Method But Not in REF, for the Trends From Table 3[a]

Resolution	OA1°1°	OA3°1°	OA3°3°	OA6°1°	OA6°3°	OA6°6°	NN
0.5° 15d common					0.0		
Ratio					3		
0.5° 30d common							
Ratio							
0.5° 60d common		0.0	2.6	1.8	5.8		
Ratio		481	57	142	35		
1° 15d common							
Ratio							
1° 30d common							
Ratio							
1° 60d common		0.0	4.2		13.2	4.0	
Ratio		74	21		67	14	
2° 15d common							
Ratio							
2° 30d common							
Ratio							
2° 60d common		4.2	11.9	12.5	33.2	63.9	4.0
Ratio		17	6	32	5	2	37

[a]Only significant trends are indicated.

(Figure 8). Even at the optimum, lowest temporal resolution of 60 days, OA6°6° returns no accurate value in these regions more than 50% of the time. In contrast, most of the Antarctic Circumpolar Current region (60°S–45°S) and Pacific sector have inaccurate values less than 30% of the time (Figure 8). Although there are still areas of the Southern Ocean where OA6°6° cannot return accurate values throughout the 10 years of the Argo period (2005–2014), it is by far a better method than OA1°1° and NN, even at low resolutions, to map large-scale features of the Southern Ocean and obtain values for most of the ocean.

To summarize, the best method to use depends on what is to be studied. NN is easy to implement and performs the calculation rapidly. It is adapted to the study of relatively small regions of the Southern Ocean with a good data coverage and will produce its best maps at coarse spatial resolutions. In contrast, our results suggest that OA with large decorrelation radii is the most appropriate for the study of a basin or the whole Southern Ocean, as was done by *Boehme et al.* [2008] or *Ren et al.* [2011] for example. Low decorrelation radii return values that are slightly more accurate, but for a significantly smaller fraction of the Southern Ocean. For optimum results, we also recommend low temporal resolutions (60 days), for the more points are included in the search radius the more accurate the method is. As the spatial resolution has little effect on the performances of OA, which is instead controlled by its decorrelation radii, and since high-resolution maps are significantly heavier and longer to run, we recommend the use of low spatial resolutions (1 or even 2°). Regarding the study of the interannual variability in the Southern Ocean, we would recommend the use of OA6°6°. We next examine whether it also the best method for the study of possible trends in the MLD.

4.2. Trends

Another important use of hydrographic data is for the detection of oceanic trends, mostly in relation to climate change. To see the impact of scattered data and re-mapping on trends, we study whether the

Table 5. Trends and Their 95% Confidence Interval (in m yr^{-1}) in Annual Mean MLD in the Indian Ocean[a]

Resolution	REF	OA1°1°	OA3°1°	OA3°3°	OA3°1°	OA6°3°	OA6°6°	NN
0.5° 15d	−1.07 ± 0.41		2.84 ± 1.46	3.16 ± 0.60		−1.48±0.33*	−1.60±0.54*	
0.5° 30d	−1.06 ± 0.42			−1.15±0.58*	−2.23 ± 0.77	−1.51±0.40*	−1.69±0.68*	
0.5° 60d	−1.06 ± 0.41			−1.66±0.69*	−2.15 ± 0.64	−1.82±0.59*	−1.86±0.53*	
1° 15d	−1.16 ± 0.48			2.65 ± 0.81		−1.41±0.35*	−1.65 ± 0.50	
1° 30d	−1.16 ± 0.48				−3.29 ± 0.81	−1.29±0.24*	−1.71±0.68*	
1° 60d	−1.16 ± 0.48			−1.41±0.61*	−2.55 ± 0.35	−1.90±0.37*	−1.83±0.61*	
2° 15d	−1.08 ± 0.26					−1.82 ± 0.23	−1.62±0.43*	
2° 30d	−1.08 ± 0.26					−1.57±0.68*	−2.15 ± 0.62	
2° 60d	−1.08 ± 0.26					−1.89 ± 0.51	−1.62±0.55*	

[a]Only significant trends are indicated. A star ⋆ indicates that there is a partial overlap between the REF and method's intervals.

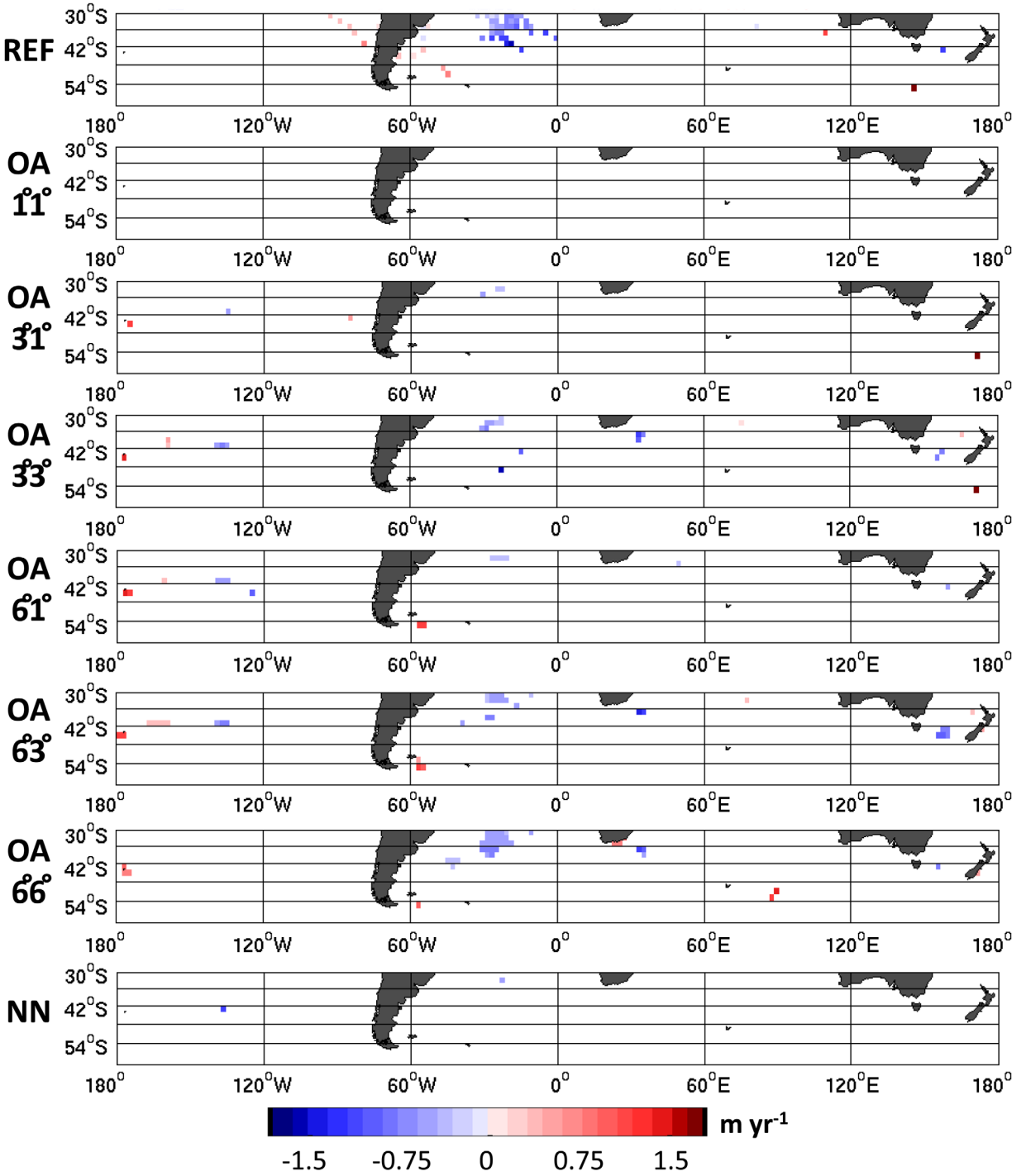


Figure 10. Significant trends in the Southern Ocean (60°S–30°S) in summer MLD, resolution 2° and 60 days, for the model (REF), all six objective analyses OA (first number indicates the decorrelation radius in longitude, second number in latitude) and NN.

methods NN and OA (all radii considered) can reproduce possible trends that exist in the model over the 10 year period. We will not discuss whether such trends in the model are realistic as it is not the focus of this paper. Trends were computed at each grid point by simple linear regression for the annually average MLD, the time series of summer MLD only and the time series of winter MLD only, thus on series composed on 10 points (with as many degrees of freedom, considering that the decorrelation time scale for a signal such as the MLD is much shorter than a year). Statistical significance of the slopes was tested at the 95% level. We

Table 6. Same as Table 4 for the Trends From Table 5 (Annual Mean MLD)[a]

Resolution	OA1°1°	OA3°1°	OA3°3°	OA6°1°	OA6°3°	OA6°6°	NN
0.5° 15d common		0.0	0.0		2.3	10.0	
Ratio		75	75		4	0.3	
0.5° 30d common			0.3	0.3	6.4	6.0	
Ratio			Inf	Inf	1	0.5	
0.5° 60d common			1.0	0.3	4.1	3.6	
Ratio			21	11	1	1	
1° 15d common			0.0		3.0	10.3	
Ratio			22		2	0.4	
1° 30d common				0.0	5.1	6.2	
Ratio				22	3	1	
1° 60d common			1.0	0.0	2.1	3.1	
Ratio			Inf	11	6	2	
2° 15d common					0.0	8.4	
Ratio					2	0.4	
2° 30d common					0.0	8.4	
Ratio					5	0.6	
2° 60d common					4.2	8.4	
Ratio					1	1	

[a]Only significant trends are indicated. Inf indicates that the second area is equal to zero.

found two significant trends in the model: a negative trend in summer MLD in the Atlantic Ocean, and a negative trend in annual mean MLD in the Indian Ocean (Figure 9). Not only are these two trends interesting because they are located in different basins, but also they have a similar magnitude (on average -0.6 m yr^{-1} in the Atlantic, -1.1 m yr^{-1} in the Indian, from the data set degraded at a resolution of 2° and 60 days) yet a different extent. The area in the Atlantic is about 6 times as large as the area in the Indian Ocean (Figure 9).

For all mapping methods, we consider any significant trend in the summer MLD in the Atlantic Ocean (45°S–30°S and 45°W–5°E as in Figure 9) and in the annual mean MLD in the central Indian Ocean (45°S–30°S and 50°E–70°E as in Figure 9). These trends are considered not significantly different from that of the original model REF if their 95% confidence intervals partially overlap. Such trends are indicated with a star $\star$ in Tables 3 and 5. Regarding the summer time series in the Atlantic (Table 3), OA1°1° never has any trend and NN displays a trend in the 2° horizontal resolution and 60 days case only. Most other methods (OA3°1° through OA6°6°) have a trend for all spatial resolutions with a temporal resolution of 60 days, but they tend to underestimate the magnitude compared with REF (first column of Table 3). All the trends for the resolution 60 days are not significantly different from that of REF, mostly because the trend in REF has a large uncertainty. The methods OA3°1° to OA6°6° also largely underestimate the area over which there is a trend (Table 4): the common area with REF is small, and the area in the model is 1 order of magnitude larger than in the method. Only OA6°6° in the lowest resolution 2° and 60 days has a relatively large common area, and similar areas in REF and the method (slightly shifted southward for OA6°6°, see Figure 10).

In the Indian Ocean, the trend in annual mean MLD in contrast is overestimated, detected for all resolutions but for less methods (Table 5). NN and OA1°1° have no significant trend over the area where the model has a trend. OA3°1°, OA3°3°, and OA6°1° have a trend of the correct sign in less than half of the cases, often significantly different from that of REF (few $\star$ in Table 5), and over very small areas (Table 6). No consistent behavior can be found between OA6°3°, OA6°6°, the resolutions and the magnitude of the trend. Regarding the areas over which there is a trend, OA6°3° underestimates them at high temporal resolution while OA6°6° overestimates them, but both methods have the same area as REF for a resolution of 60 days (Table 6). For both the summer MLD in the Atlantic (Table 3) and the mean annual MLD in the Indian Ocean (Table 5), the trends are best represented using large decorrelation radii and low temporal resolutions.

In some cases, the mapping methods shown here succeed in reproducing the trend that is present in the original data. However, problems would arise if these methods were also creating fake trends in locations where the original data had none. We assess all the significant trends in the re-mapped annual minimum MLD north of the ice-covered regions (Figure 10 for 2° and 60 days), and see that there are trends in all three basins. For a given resolution, larger decorrelation radii give more homogeneous patterns, whereas small radii have a number of small scattered areas with trends (Figure 10). One pattern that appears for

Table 7. Unrealistic Negative Trends and Their 95% Confidence Interval (in m yr^{-1}) in Summer MLD in the Western Pacific Ocean and Areas Over Which They Occur (in 10,000 km^2)[a]

Resolution	OA1°1°	OA3°1°	OA3°3°	OA6°1°	OA6°3°	OA6°6°	NN
0.5° 15d				−1.08 ± 0.09	−0.94 ± 0.08		
Area				0.9	2.9		
0.5° 30d				−0.82 ± 0.12	−0.86 ± 0.13		
Area				3.2	6.4		
0.5° 60d	−0.50 ± 0.32	−0.50 ± 0.18	−0.60 ± 0.14	−0.58 ± 0.21	−1.03 ± 0.35		
Area	0.2	2.9	12.4	8.6	1.8		
1° 15d				−1.01 ± 0.18	−0.96 ± 0.17		
Area				1.0	7.2		
1° 30d				−0.67 ± 0.12	−0.76 ± 0.10		
Area				5.9	4.9		
1° 60d		−0.46 ± 0.06	−0.52 ± 0.05	−0.79 ± 0.02	−0.28 ± 0.03		
Area		0.9	8.4	2.7	2.1		
2° 15d							
Area							
2° 30d					−1.12 ± 0.27	−0.77 ± 0.20	
Area					4.0	3.9	
2° 60d		−0.45 ± 0.30	−0.56 ± 0.09	−0.58 ± 0.21	−0.60 ± 0.05		−1.02 ± 0.42
Area		3.8	11.4	14.9	11.4		3.7

[a]Only significant trends are indicated.

most methods is the negative trend in the western Pacific Ocean (Figure 10 and Table 7). No consistent link can be found between the magnitude of this spurious trend and the resolution, although the trend tends to be less strong for 60 days. However, it occurs over larger areas (last row of Table 7). As was found for the Atlantic, NN has a trend in the Pacific with the lowest resolution only (2° and 60 days, Table 7). This suggests that at high resolutions, NN does not return values at all grid cells often enough (Figure 8) for a significant trend to be found. There is no consistent link between the value of the decorrelation radii and the magnitude or area of the unrealistic trend, with OA6°1° and OA6°3° having the largest occurrences.

In summary, our analyses suggest that 10 years of observations still is too short a period to try and detect possible trends in the Southern Ocean MLD, in particular considering that the number of floats has only been roughly constant for 5 years. Both methods NN and OA (with all the decorrelation radii tested) suffer from the same biases: there is no resolution at which they reproduce the existing trends (correct magnitude and area) without creating any unrealistic one as well. Rather than mapping scattered data to systematically detect trends, it seems more advisable to work with individual profiles that can be found at the same location through the last decades, as done for example by *Gille* [2008]. Note that the trends in MLD were relatively small in this study; maybe larger trends and/or over a larger area could be mapped more easily.

5. Conclusions

We have shown in this paper that all the methods we tested, inspired from the current literature (Table 1), at all the resolutions, introduce biases into the original data set. The more points are considered or available, the least biased the re-mapped field is. This is particularly adapted to the production of climatologies [e.g., *de Boyer Montégut et al*., 2004; *Dong et al*., 2008; *Locarnini et al*., 2013]. Here the methods were most accurate at low temporal resolution, ideal for the study of seasonal time series [*Ren et al*., 2011]. NN worked best at low spatial resolution (more points to consider), but returned overall a poor filling rate, as the search was limited to immediate grid cells in our application. The OAs were more accurate with low decorrelation radii (less smoothing), such as those used by *Sallée et al*. [2008]. Although less accurate, OA was most powerful at mapping large areas of the Southern Ocean with the largest decorrelation radii of 6° both in longitude (as used by *Ren et al*. [2011]) and in latitude (larger than what is used in the current literature).

To study the interannual variability of the MLD in the whole Southern Ocean from scattered Argo measurements, our results suggest the use of an objective analysis mapping method, with both decorrelation radii equal to 6° and a target time resolution of 60 days, which gives the best compromise between accuracy and filling rate (Figure 8g). Outside of the ice-covered region, it has a year-round area-weighted mean error of −9 m (largest error of −83 m), that is the MLD is not deep enough. This error reaches −31 m (maximum

−288 m) in winter and +10 m (+67 m) in summer when the MLD is too deep. Such recommendation can probably be extended to other upper ocean properties to be mapped with the current hydrographic database (e.g., mixed-layer salinity and temperature), although distinctive space-time statistics of each field may have some impact on these results.

No method was adapted to reconstruct statistically significant decadal trends. For all the resolutions tested, the method that can reproduce existing MLD trends also create unrealistic trends somewhere else, a result possibly sensitive to the weakness of the trends in the MLD field. We recommend the use of methods similar to that of *Gille* [2008], which is following specific profiles through time, rather than trying to map the whole Southern Ocean to study its trends.

We did not test any "improved" OA, that is an OA with geographical decorrelation (as here) but also an extra decorrelation term controlled by a physical parameter, such as potential vorticity [*Boehme et al*., 2008] or changes in properties representative of fronts [*Schmidtko et al*., 2013]. Such an improved method should, in theory, prevent neighboring distinct water masses to be artificially mixed during the mapping. In practice, the implementation of such a method is a long and complex tuning process. First, the physical parameter needs to be used for mapping without the geographical constraints to assess its optimum corresponding decorrelation radius. Then both physical and geographical criteria have to be assigned weights. The implementation of such a method proved beyond the scope of this paper. However, we hope that future method description papers will give more details regarding the choices of parameters made, rather than simply stating that they were "optimum."

Finally, the main source of biases for the methods used here is the lack of observational data points. Even the best method, OA6°6°, is unable to accurately represent some sectors of the subtropical Atlantic, Indian, and Pacific Oceans a third of the time. Obviously, most of the ice-covered region around Antarctica cannot be represented accurately all of the time, as Argo floats have only been deployed in ice-free regions to date, but these regions have recently started being sampled using elephant-seals [e.g., *Roquet et al*., 2014]. It does mean that so far, efforts to assess ocean properties and their changes around Antarctica, critical to correctly project Antarctic basal melt, rely on scarce, sporadic ship measurement [*Schmidtko et al*., 2014]. Similarly, recent studies have highlighted the nonnegligible contribution of Antarctic Bottom Water to current and future global sea level rise [*Kuhlbrodt and Gregory*, 2012; *Purkey and Johnson*, 2013; *Heuzé et al*., 2015], yet the current generation of Argo floats in the Southern Ocean cannot be used to study this water mass as they are limited to the top 2000 m of the ocean. Hopefully the deployment of deep Argo in the coming decade will fill this gap and allow for a full-depth, high-resolution mapping of the whole Southern Ocean.

Acknowledgments

Support for this research was provided by CNES as part of the OSTST "MISO" project (Mixed-layer Interannual variability in the Southern Ocean). The DRAKKAR simulation was performed at the Centre Informatique National de l'Enseignement Supérieur (CINES) under a GENCI allocation. DRAKKAR is supported by an International Coordination Network (GDRI) established between CNRS, NOCS, GEOMAR in Kiel, and IFREMER. The authors would like to thank the two anonymous reviewers whose comments notably improved the quality of this paper. The simulation can be obtained by contacting any of the coauthors from the CNRS-LGGE. Computations discussed in this paper were carried out on the High Performance Computing Cluster supported by the Research and Specialist Computing Support service at the University of East Anglia, UK. Any additional data or script can be obtained by contacting C. Heuzé (celine.heuze@gu.se).

Notation

MLD	mixed-layer depth.
NN	nearest neighbor.
OA	objective analysis.
OHC	ocean heat content.
PV	potential vorticity.
SSH	sea surface height.
S	salinity.
T	temperature.

References

Blanke, L., and P. Delecluse (1993), Variability of the tropical Atlantic Ocean simulated by a general circulation model with two different mixed-layer physics, *J. Phys. Oceanogr.*, *23*, 1363–1388, doi:10.1175/1520-0485(1993)023,1363:VOTTAO.2.0.CO;2.

Boehme, L., M. Meredith, S. Thorpe, M. Biuw, and M. Fedak (2008), Antarctic Circumpolar Current frontal system in the South Atlantic: Monitoring using merged Argo and animal-borne sensor data, *J. Geophys. Res.*, *113*, C09012, doi:10.1029/2007JC004647.

Bretherton, F., R. Davis, and C. Fandry (1976), A technique for objective analysis and design of oceanographic experiments applied to MODE-73, *Deep Sea Res. Oceanogr. Abstr.*, *23*, 559–582, doi:10.1016/0011-7471(76)90001-2.

de Boyer Montégut, C., G. Madec, A. Fischer, A. Lazar, and D. Iudicone (2004), Mixed layer depth over the global ocean: An examination of profile data and a profile-based climatology, *J. Geophys. Res.*, *109*, C12003, doi:10.1029/2004JC002378.

Dee, D. P., et al. (2011), The ERA-Interim reanalysis: Configuration and performance of the data assimilation system, *Q. J. R. Meteorol. Soc.*, *137*, 553–597, doi:10.1002/qj.828.

Dong, S., J. Sprintall, S. T. Gille, and L. Talley (2008), Southern ocean mixed-layer depth from Argo float profiles, *J. Geophys. Res.*, *113*, C06013, doi:10.1029/2006JC004051.

Dunn, J. R., and K. R. Ridgway (2002), Mapping ocean properties in regions of complex topography, *Deep Sea Res., Part I*, *49*, 591–604, doi:10.1016/S0967-0637(01)00069-3.
Dussin, R., B. Barnier, and L. Brodeau (2014), The making of Drakkar forcing set DFS5, *DRAKKAR/MyOcean Rep*. [Available at http://www.drakkar-ocean.eu/forcing-the-ocean/the-making-of-the-drakkar-forcing-set-dfs5].
Gille, S. (2008), Decadal-scale temperature trends in the southern hemisphere ocean, *J. Clim.*, *21*, 4749–4755, doi:10.1175/2008JCLI2131.1.
Good, S., M. Martin, and N. Rayner (2013), EN4: Quality controlled ocean temperature and salinity profiles and monthly objective analyses with uncertainty estimates, *J. Geophys. Res. Oceans*, *118*, 6704–6716, doi:10.1002/2013JC009067.
Helm, K. P., N. L. Bindoff, and J. A. Church (2010), Changes in the global hydrological-cycle inferred from ocean salinity, *Geophys. Res. Lett.*, *37*, L18701, doi:10.1029/2010GL044222.
Heuzé, C., K. J. Heywood, D. P. Stevens, and J. K. Ridley (2015), Changes in global ocean bottom properties and volume transports in CMIP5 models under climate change scenarios, *J. Clim.*, *28*, 2917–2944, doi:10.1175/JCLI-D-14-00381.1.
Holte, J., and L. Talley (2009), A new algorithm for finding mixed layer depth with applications to Argo data and subantarctic mode water formation, *J. Atmos. Oceanic Technol.*, *26*, 1920–1939, doi:10.1175/2009JTECHO543.1.
Ingleby, B., and M. Huddleston (2007), Quality control of ocean temperature and salinity profiles—Historical and real-time data, *J. Mar. Syst.*, *65*, 158–175, doi:10.1016/j.jmarsys.2005.11.019.
Juza, M., T. Penduff, J.-M. Brankart, and B. Barnier (2012), Estimating the distortion of mixed layer property distributions induced by the Argo sampling, *J. Oper. Oceanogr.*, *5*, 45–58, doi:10.1080/1755876X.2012.11020131.
Kuhlbrodt, T., and J. M. Gregory (2012), Ocean heat uptake and its consequences for the magnitude of sea level rise and climate change, *Geophys. Res. Lett.*, *39*, L18608, doi:10.1029/2012GL052952.
Le Sommer, J., T. Penduff, S. Theetten, G. Madec, and B. Barnier (2009), How momentum advection schemes influence current-topography interactions at eddy permitting resolution, *Ocean Modell.*, *29*, 1–14, doi:10.1016/j.ocemod.2008.11.007.
Locarnini, R. A., et al. (2013), *World Ocean Atlas 2013, Volume 1: Temperature*, edited by S. Levitus and A. Mishonov, *NOAA Atlas NESDIS 73*, 40 pp. [Available at https://www.nodc.noaa.gov/OC5/woa13/pubwoa13.html.]
Lyman, J., and G. Johnson (2008), Estimating annual global upper-ocean heat content anomalies despite irregular in situ ocean sampling, *J. Clim.*, *21*, 5629–5641, doi:10.1175/2008JCLI2259.1.
Madec, G. (2008), *NEMO Ocean General Circulation Model Reference Manual*, edited by S. Levitus, LOCEAN/IPSL, Paris.
Penduff, T., J. Le Sommer, B. Barnier, A.-M. Treguier, J.-M. Molines, and G. Madec (2007), Influence of numerical schemes on current-topography interactions in 1/48 global ocean simulations, *Ocean Sci.*, *3*, 509–524, doi:10.5194/os-3-509-2007.
Purkey, S., and G. Johnson (2013), Antarctic bottom water warming and freshening: Contributions to sea level rise, ocean freshwater budgets, and global heat gain, *J. Clim.*, *26*, 6105–6122, doi:10.1175/JCLI-D-12-00834.1.
Ren, L., K. Speer, and E. Chassignet (2011), The mixed layer salinity budget and sea ice in the Southern Ocean, *J. Geophys. Res.*, *116*, C08031, doi:10.1029/2010JC006634.
Roemmich, D., G. C. Johnson, S. Riser, R. Davis, J. Gilson, W. B. Owens, S. L. Garzoli, C. Schmid, and M. Ignaszewski (2009), The Argo program: Observing the global ocean with profiling floats, *Oceanography*, *22*, 34–43, doi:10.1029/10.5670/oceanog.2009.36.
Roquet, F., et al. (2014), A Southern Indian Ocean database of hydrographic profiles obtained with instrumented elephant seals, *Nat. Sci. Data*, *1*, 1:140028, doi:10.1038/sdata.2014.28.
Sallée, J.-B., K. Speer, and R. Morrow (2008), Response of the Antarctic Circumpolar Current to atmospheric variability, *J. Clim.*, *21*, 3020–3039, doi:10.1175/2007JCLI1702.1.
Sallée, J.-B., K. Speer, S. Rintoul, and S. Wijffels (2010), Southern Ocean thermocline ventilation, *J. Phys. Oceanogr.*, *40*, 509–529, doi:10.1175/2009JPO4291.1.
Santer, B. D., T. M. L. Wigley, J. S. Boyle, D. J. Gaffen, J. J. Hnilo, D. Nychka, D. E. Parker, and K. E. Taylor (2000), Statistical significance of trends and trend differences in layer-average temperature time series, *J. Geophys. Res.*, *105*, 7337–7356, doi:10.1029/1999JD901105.
Schmidtko, S., G. Johnson, and J. Lyman (2013), MIMOC: A global monthly isopycnal upper–ocean climatology with mixed layers, *J. Geophys. Res. Oceans*, *118*, 1658–1672, doi:10.1002/jgrc.20122.
Schmidtko, S., K. Heywood, A. Thompson, and S. Aoki (2014), Multidecadal warming of Antarctic waters, *Science*, *346*, 1227–1231, doi:10.1126/science.1256117.
Taylor, K. (2001), Summarizing multiple aspects of model performance in a single diagram, *J. Geophys. Res.*, *106*, 7183–7192, doi:10.1029/2000JD900719.
Uppala, S. M., et al. (2005), The ERA-40 reanalysis, *Q. J. R. Meteorol. Soc.*, *131*, 2961–3012, doi:10.1256/qj.04.176.
Vivier, F., D. Iudicone, F. Busdraghi, and Y.-H. Park (2010), Dynamics of sea-surface temperature anomalies in the Southern Ocean diagnosed from a 2D mixed-layer model, *Clim. Dyn.*, *34*, 153–184, doi:10.1007/s00382-009-0724-3.